Fatigue strength of misaligned non-load-carrying cruciform joints made of ultra-high-strength steel

Ahola Antti, Björk Timo

DOI: 10.1016/j.jcsr.2020.106334

Fatigue strength of misaligned non-load-carrying cruciform joints made of ultra-high-strength steel

A. Ahola*, T. Björk

Laboratory of Steel Structures, School of Energy Systems, Lappeenranta-Lahti University of Technology LUT, P.O. Box 20, FI-53851 Lappeenranta, Finland

ABSTRACT

Misalignments and distortions in welded plate components act as stress raisers and can significantly decrease the fatigue strength of welded connections. This paper investigates the effect of the plate misalignment of transverse attachments on the fatigue behavior of axially-loaded non-load-carrying cruciform (NLCX) joints. Experimental fatigue tests with and without the plate misalignment are carried out for fillet-welded NLCX joints. The test specimens were fabricated of S1100 ultra-high-strength steel grade, and the fatigue tests were conducted using an applied stress ratio of R = 0.1. Numerical finite element analyses were conducted to obtain the stress concentrations induced by the misalignment. In addition, varied geometry parameters were applied to investigate their effect on the magnitude of stress concentrations. Stress concentrations were obtained using the structural hot spot stress method applying linear surface extrapolation and 1 mm below depth methods, and the effective notch stress concept with the reference radius of 1 mm. Experimental fatigue tests showed a decrease of up to 12% in fatigue strength depending on the degree of misalignment. The highest stress concentration was induced when the misalignment to the joint width ratio was e/L = 0.2–0.4. Structural stresses cannot be estimated using the linear surface extrapolation. Instead, structural stress at the 1 mm depth and effective notch stress concept accurately evaluated the misalignment effect on the fatigue performance of NLCX joints, and provided a good correspondence between the theoretical and experimental fatigue strength estimations.

Keywords: fatigue; welded joint; misalignment; fillet weld; ultra-high-strength steel; 4R method

* Corresponding author: Antti Ahola (antti.ahola@lut.fi)

1 INTRODUCTION

Use of high- and ultra-high-strength steels (HSS/UHSS) in welded steel constructions enables weight reduction with similar static strength capacity, unlike their counterparts manufactured from mild steel. Consequently, HSS and UHSS materials prove profitable particularly in weight-critical structures and devices to increase payloads, e.g. in the fields of civil engineering, transportation, lifting and the automotive industry [1]. Such structures are typically subjected to fluctuating or cyclic load conditions, making them susceptible to fatigue failures. Whereas it is well-known in the prior art that increasing the static strength capacity of steel material does not contribute to high fatigue strength in welded components [2–4] unless specific post-weld treatments, see e.g. [5,6], are employed to improve the fatigue strength. On the other hand, a decrease in plate thickness predisposes UHSS components for different manufacturing imperfections, particularly those associated with welded details, i.e. welding deformations and the assembly accuracy of plate components. Structural misalignments and macrogeometric imperfections act as stress raisers, which may drastically decrease the fatigue strength capacity of welded joints and, thus, necessitate the consideration of fatigue performance in welded UHSS components.

The consideration of different misalignments and imperfections has been addressed in design codes and guidelines [7–9] providing parametric equations to analyze structural stress concentrations, typically denoted with k_m or k_s factors. In recent studies, significant interest has been placed on butt-welded details. Indeed, several studies have been conducted to consider misalignments in the structural HS system [10–12] but SCFs based on notch stress concepts have also been under investigation [13–15]. In cruciform joints with double-sided fillet welds and subjected to axial loading in the adjoined plate components – see Fig. 1a, i.e. in the case of load-carrying X-joints (LCX) – the effect plate and angular misalignments on fatigue performance and failure location have been well recognized in prior investigations [16–20]. Together with these plate misalignments, the fatigue behavior of the LCX joints is influenced by the size of weld throat thickness, the depth of weld

penetration, potentially conducted post-weld treatments at the weld toes [21], residual stress state [22], and loading type [23,24].

Although extensive research has been carried out on the misalignment of LCX joints, far too little attention has been paid to the effect of the plate misalignment of transverse attachments in similar cruciform joints but subjected to axial loading at the base plate, i.e. non-load-carrying cruciform (NLCX) joints, see Fig. 1b. Henceforth in this paper, the term 'plate misalignment' signifies the misalignment of transverse attachments of NLCX joints. In such components, the misalignment can be introduced as a result of manufacturing inaccuracy, or design and functional purposes. The fatigue failure in a misaligned NLCX joint typically occurs, as also demonstrated in this study, at the inner weld toe. In recent studies, Zong et al. [25] and Su et al. [26] conducted numerical analyses based on linear elastic fracture mechanics (LEFM) to explore the effect of NLCX joint plate misalignment on fatigue strength capacity. In both studies [25,26], a relatively small degree of the misalignment was investigated, i.e. maximum of e = 3 mm for plate thicknesses of 8 mm and 12 mm, respectively, and a fatigue-life decrease of approximately 10% was found due to such misalignment. Some insights on the topic can also be found in [27]. In thin-walled UHSS components, relatively higher misalignments can potentially occur. Moreover, in UHSS weldments in the as-welded condition, the crack initiation time might become predominant in terms of total fatigue life [28,29] and, in such cases, fatigue strength assessment using LEFM might significantly underestimate the capacities. Furthermore, the lack of experimental data on the fatigue strength of misaligned NLCX joints restricts further conclusions being made on the issue.

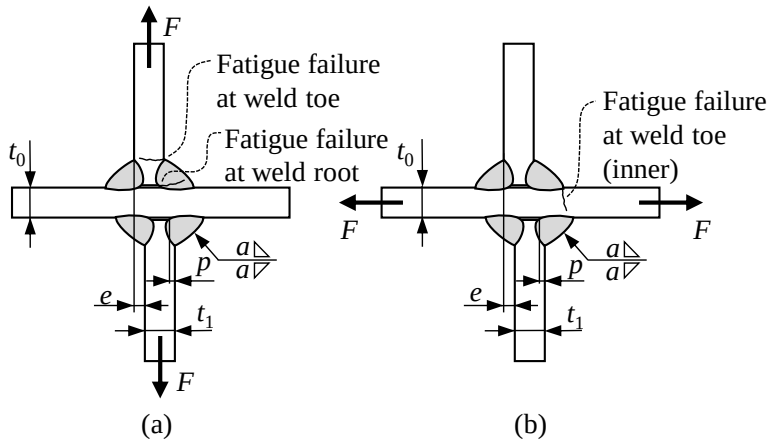

Fig. 1. Potential fatigue failure paths in axially loaded (a) LCX joint with plate misalignment and (b) NLCX joint with plate misalignment.

This study aims to experimentally and numerically investigate how plate misalignment affects stress concentrations using different fatigue design criteria, i.e. structural HS stress and ENS concepts, together with what the efficient methods are for assessing the fatigue strength of a UHSS NLCX joint with plate misalignment. Finite element (FE) analyses are carried out to numerically investigate the structural and notch SCFs introduced by the plate misalignment in fillet-welded NLCX joints. Stress distributions along the base plate from the weld toe are obtained, and the structural stresses are obtained using linear surface extrapolation (LSE) method [30], and 1 mm below the surface approach, most commonly recognized as the Xiao–Yamada method [31]. For comparison, the effective notch stress (ENS) concept with a reference radius of r_{ref} = 1.0 mm [32] is employed to evaluate the fatigue effective notch stress. Subsequently, the numerically obtained findings on the effects of the plate misalignment are verified by conducting experimental fatigue tests on fillet-welded NLCX joints made of t = 8 mm S1100 UHSS steel plates prepared with and without plate misalignment. The *S-N* curves for joints with a different degree of plate misalignment are evaluated using different stress criteria, i.e. the nominal stress, structural HS stress and ENS concepts, and efficient methods for evaluating the effect of plate misalignment are addressed. This study is limited to NLCX joints for

which the transverse attachments are unconstrained and so will not carry any axial forces or suffer bending moments.

2 MATERIALS AND METHODS

2.1 Experimental fatigue tests

2.1.1 Specimen design and preparation

Experimental fatigue tests were carried out for NLCX joints made of S1100 UHSS plates with the base and adjoined plate thicknesses of $t_0 = t_1 = 8$ mm, respectively. Union X96 (Ø1.0 mm) solid wire was used in the gas metal arc welding (GMAW) of the test specimens. Fig. 2 shows the shape and dimensions of the test specimens, and Table 1 and Table 2 present the mechanical properties and chemical compositions of the studied materials, respectively.

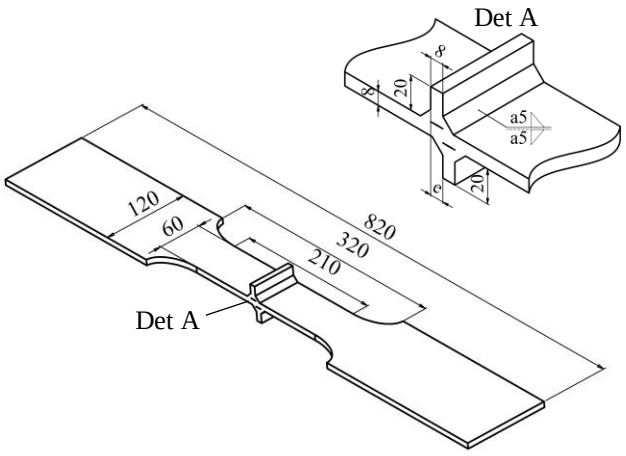

Fig. 2. Shape and dimensions of the test specimens (all dimensions in mm).

Table 1. Mechanical properties of the studied materials (nominal values).

Material	Proof strength $R_{p0.2,min}$ [MPa]	Ultimate strength R_m [MPa]	Elongation $A_{5,min}$ [%]	Impact Energy KV [J] (at temp.)
S1100	1100	1130-1350	10	27 (-40°C)
Union X96[1]	930	≥980	14	47 (-50°C)

[1]Mechanical properties of undiluted weld metal

Table 2. Chemical compositions of the studied materials (nominal values).

Material	C_{max}	Si_{max}	Mn_{max}	P_{max}	S_{max}	Al_{min}
S1100	0.20	0.50	1.80	0.02	0.005	0.015
	C_{max}	Si_{max}	Mn_{max}	Cr_{max}	Ni_{max}	Mo_{max}
Union X96[1]	0.12	0.8	1.9	0.45	2.35	0.55

[1]Chemical composition of undiluted weld metal

As the aim of this study is to investigate the effect of plate misalignment on the fatigue strength of NLCX joints made of UHSS, the misalignments in the test specimens were intentionally produced. A preliminary numerical FE analysis study on the stress concentrations induced by the plate misalignment, observed at the structural stress (LSE method) and notch stress (ENS method, r_{ref} = 1.0 mm) level, was carried out to choose misalignment levels. The model details regarding the FE analysis correspond to the specifications given in Section 2.2.1, and the analyses were carried out for $t_0 = t_1 = 8$ mm with four symmetric welds with a throat thickness of $a = 5$ mm, and no weld penetration was assumed. Fig. 3 shows the SCFs in terms of structural HS stress (K_s) and ENS (K_{tot}) as a function of plate misalignment. Fig. 3 reveals that the maximum structural SCF ($K_{s,max}$) and notch SCF ($K_{tot,max}$, including both structural and notch stress) occur at the different degree of misalignment. The notch SCF accounts for the geometrical symmetry at the joint section, while structural SCF depends on the position of neutral axis and stress flow over the attachments. It is also worth mentioning that the structural SCFs were determined using the LSE method resulting in different structural SCFs in comparison with the Xiao-Yamada method (see Section 3.2).

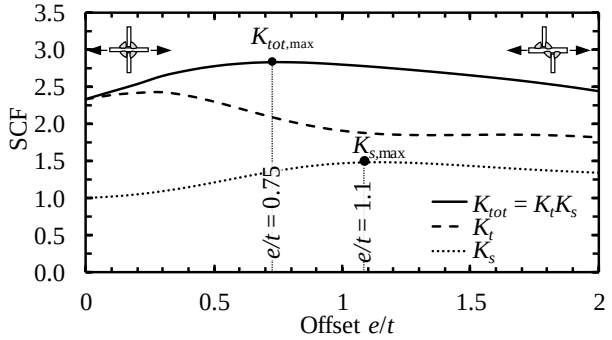

Fig 3. SCFs for NLCX joint with $t_0 = t_1 = 8$ mm and $a = 5$ mm. K_t represents pure notch SCF, i.e. the total stress divided by the structural stress.

Three different degrees of misalignment were chosen according to the FEA study, i.e. e/t = 0.75, e/t = 1.1, and e/t = 2.0 corresponding to misalignments of e = 6 mm, 9 mm and 16 mm, based on the maximum values of SCFs, see Fig. 3. In addition, the reference specimens without plate misalignment were also manufactured, with the test results were initially reported in a previous study [33]. A total number of 14 specimens were fabricated and tested, with Table 3 showing the geometry and load configuration for each. To diminish the effect of metallurgical and geometrical scatter within the test specimen, the NLCX joints were prepared using a robotic GMAW process, and the target throat thickness of a = 5 mm was applied, according to the conducted preliminary FEA study. Fig. 4 shows the GMAW preparation of test specimens and a welded specimen, with Table 4 presenting the key values of the welding specification procedure (WPS).

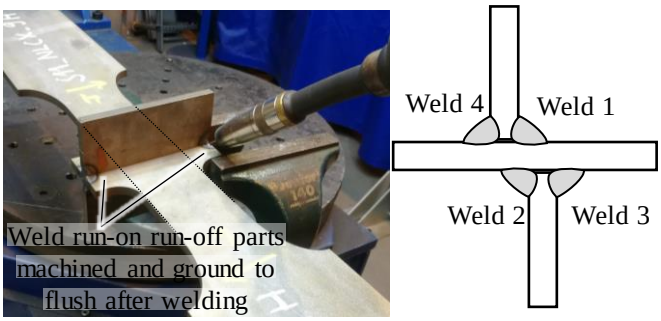

Fig. 4. (a) Welding preparation of the test specimen with a robotic GMAW and (b) sequence of welds in the misaligned specimens.

Table 3. Test matrix

Misalignment e [mm]	No. of specimens	Specimen ID
0	6	S11_NLCX_1 – 6
6	2	S11_NLCX_13 – 14
9	4	S11_NLCX_15 – 18
16	2	S11_NLCX_19 – 20

Table 4. GMAW parameters applied in the test specimen preparation. Shielding gas was Ar+8%CO_2, and travel angle and working angle were 18° (pushing) and 45°, respectively.

Voltage U [V]	Current I [A]	Travel speed v_{travel} [cm/min]	Wire feed rate v_{wire} [m/min]
28.0-28.4	235-240	35.4	13.2

2.1.2 Geometry and residual stress measurements

To evaluate the plate misalignment effect on the residual stresses, and to consider the welding quality in the joint fatigue strength assessment, residual stresses and weld geometries were determined before conducting the fatigue tests. Residual stresses were measured using an X-ray diffractometer (XRD, Stresstech X3000 G3 device) parallel to the loading direction. The collimator's spot size was 1 mm and the exposure time was 40 seconds. The average scatter of the residual stress measurements (including all points) was ±20 MPa. Residual stress distributions along the specimens' longitudinal direction were obtained in one reference specimen and one misaligned specimen. In the rest of the specimens, only the residual stresses at weld toes were measured. In the misaligned specimens, it was assumed that the fatigue critical weld toes are weld IDs 1 and 2, see Fig. 4 welding sequence, and the residual stress measurements were only carried out at these welds. Fig. 5 shows the residual stress distributions in the longitudinal direction of a reference specimen (ID S11_NLCX_1, e = 0) and a misaligned specimen (ID S11_NLCX_15, e = 9 mm). As demonstrated in Fig. 4, no welding deformations were prevented in the test specimens and, thus, low and even compressive residual stresses were measured at the weld toes despite the specimens being in the as-welded condition, similarly to reported in Refs. [33,34].

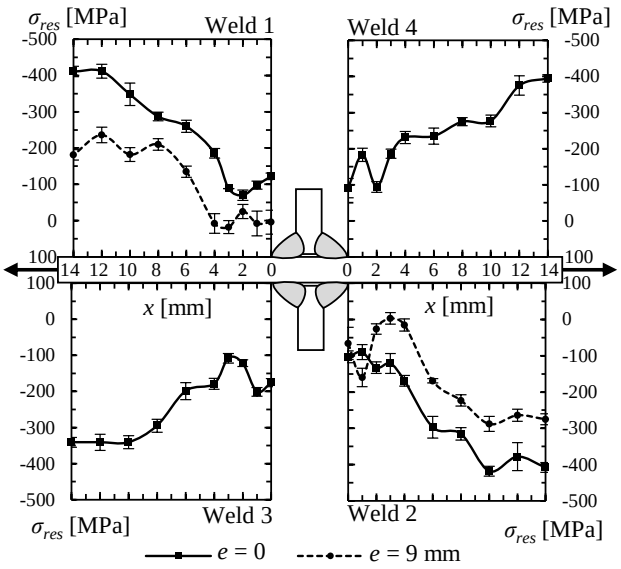

Fig. 5. Residual stress distribution and scatter values in a reference (ID S11_NLCX_1, e = 0) and a misaligned specimen (ID S11_NLCX_15, e = 9 mm).

Table 4. Summary of residual stress measurements. n/a signifies not analyzed (welds 3 and 4 were not fatigue critical).

	Residual stress σ_{res} [MPa]				
Offset	Weld 1	Weld 2	Weld 3	Weld 4	Measured specimens
e = 0	-101	-117	-129	-93	S11_NLCX_1 – S11_NLCX_4
e = 6 mm	12	-22	n/a	n/a	S11_NLCX_13 – S11_NLCX_14
e = 9 mm	4	-8	n/a	n/a	S11_NLCX_15 – S11_NLCX_18
e = 16 mm	-44	36	n/a	n/a	S11_NLCX_19 – S11_NLCX_20

The weld geometries were measured using a 2D coordinate measuring device and the weld profile determined with a laser displacement sensor and inductive displacement transducer. From these measurements, the average weld toe radius of $r_{true,avg}$ = 0.3 mm, flank angle of θ_{avg} = 44°, and external throat thickness of a_{avg} = 5.1 mm were evaluated.

2.1.3 Fatigue test set-up

Fatigue tests were carried out using a servo-hydraulic fatigue testing machine with the test frequency of f = 1–3 Hz, using a constant amplitude uniaxial loading with an applied stress ratio of R = 0.1. Fig.

6 shows the specimen attached to the test rig. The failure criterion for the fatigue tests was the total rupture of the specimen.

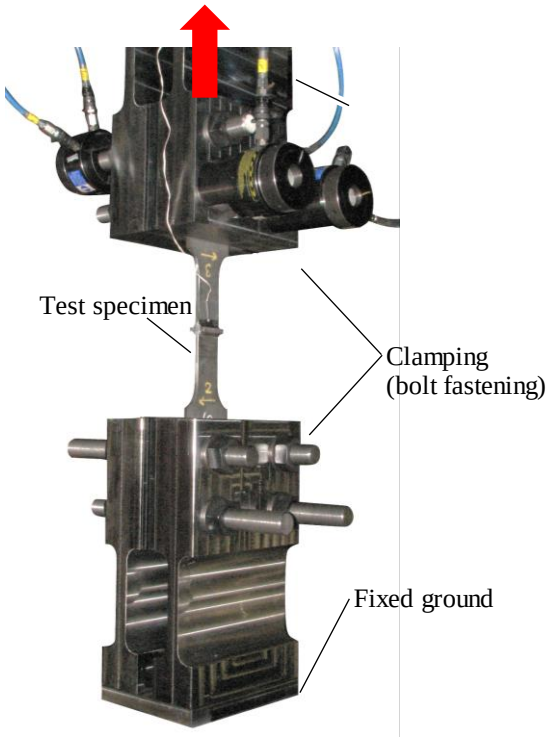

Fig. 6. Fatigue test set-up

2.2 Numerical analyses

2.2.1 Model configuration and validation

The principal aim of the numerical analyses is to obtain the stress concentration factors induced by NLCX joint plate misalignment. Following the separation of stress components into three categories, i.e. nominal stress, structural HS stress, and notch stress, the numerical analyses are carried out to obtain both structural and notch stresses. In a previous investigation [28], it was well recognized that the transverse attachment (NLCT) joint has significantly lower stress concentration than the NLCX joint. Consequently, notch and joint detail must be taken into account in the notch stress analysis, instead of only determining the structural stresses. Three different approaches are employed in the numerical study:

- Structural stress approach using the LSE method [35]
- Structural stress approach using the Xiao–Yamada method [31]

- Notch stress approach using the ENS concept (r_{ref} = 1.0 mm) [32]

As the studied joint is assumed to represent a continuous transverse joint, a two-dimensional (2D) plane strain FE model is used in the analysis to obtain the stress concentrations. The geometries of the models were obtained from the fatigue tested specimens; base and attached plate thickness of t_0 = t_1 = 8 mm, and welded with the throat thickness of a = 5.1 mm and the flank angle of θ = 44° corresponding to the measured geometries described in Section 2.1.2.

In the LSE method, two different types of hot spot stresses are presented, i.e. type 'a' and type 'b', depending on whether there is a distinct through-thickness stress distribution or not. In the misaligned NLCX joint, the division into two types is indeterminable since the increase in misalignment changes the joint type from type 'a' to type 'b'. Thus, both methods are applied in the present study. A fine mesh is applied in accordance with the guided mesh sizes [35], see FE mesh details shown in Fig. 7, and the stresses are extrapolated from the proposed distances, as follows:

$$\sigma_{hs} = 1.67\sigma_{0.4t} - 0.67\sigma_{1.0t} \quad (1)$$

$$\sigma_{hs} = 1.5\sigma_{4\,\mathrm{mm}} - 1.5\sigma_{8\,\mathrm{mm}} + \sigma_{12\,\mathrm{mm}} \quad (2)$$

For the ENS method, the reference radius of r_{ref} = 1.0 mm was applied to assume the worst-case scenario for the transition from the base material to the weld (r_{true} = 0). For the fatigue life predictions using the 4R method [33], the radius of $r = r_{true}$ + 1 mm = 0.3 mm + 1 mm = 1.3 mm, was also applied. Otherwise, the models of the 4R method correspond to those of the ENS concept. As the notch stresses have been obtained from these models, a high mesh density and quadrilateral shape of elements are required for the convergence. The FE mesh size of r/20 was applied according to the study by Baumgartner and Bruder [36].

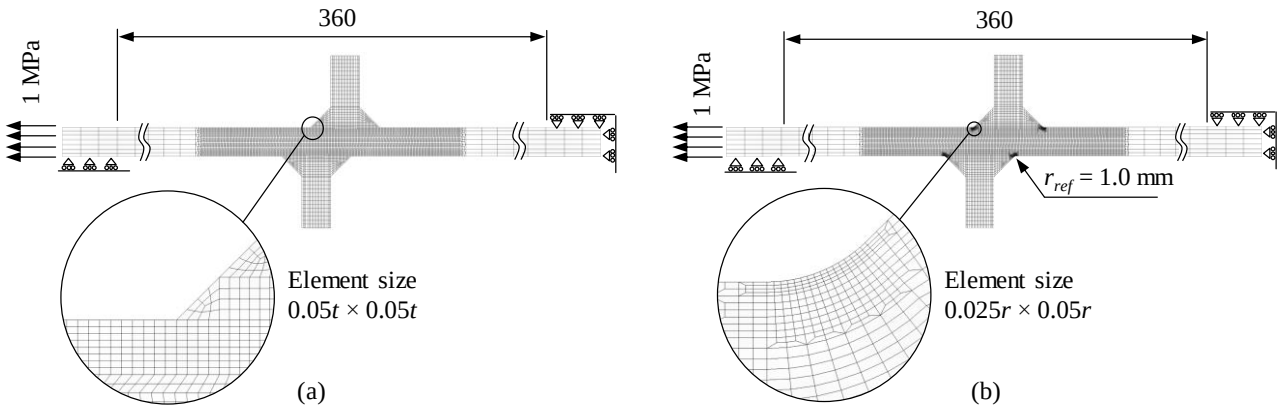

Fig. 7. FE model configurations: (a) HS models, and (b) ENS model.

2.2.2 Parametric study on the effects of geometry parameters

In section 2.2.1, the FE model geometry was specified according to the fatigue tested geometries. From these FEAs, the stress concentrations (HS and ENS methods) for the determination of *S-N* curves can be obtained. Nevertheless, it is worth noting that the magnitude of plate misalignment effect on the stress concentrations and, subsequently, on the fatigue strength of fillet-welded NLCX joints might vary based on the geometry configuration of the NLCX joint. Consequently, a parametric analysis of the effect of change in the geometry parameters on the magnitude of stress concentrations is investigated by conducting FEA.

The base plate thickness t_0 = 8 mm is held as a reference value, with the attached plate thickness and throat thickness varied. In considering a real joint configuration, the parametric study concerns are limited to only single-pass GMAW, for which a throat thickness of a = 3.0–6.0 mm can easily be reached with single-pass welding and, consequently a/t_0 ratios of 0.33, 0.50 and 0.66 were chosen for the analyses. In addition, three different plate thicknesses were tested: similar plate, and thinner and thicker plate thickness, see Fig. 8. Also, the infusible weld root width w was altered. In all cases, the fillet welds are modeled with a 45° flank angle. As a result, 27 geometry combinations are achieved, and when the plate misalignment was modeled using a 0.8 mm step size with a total number of 35 increments for each geometry combination (constant step size was used to simplify the element mesh

modeling) from the ratios of e/L = 0 to e/L = 1. A total number of 1890 element models and analysis results are obtained.

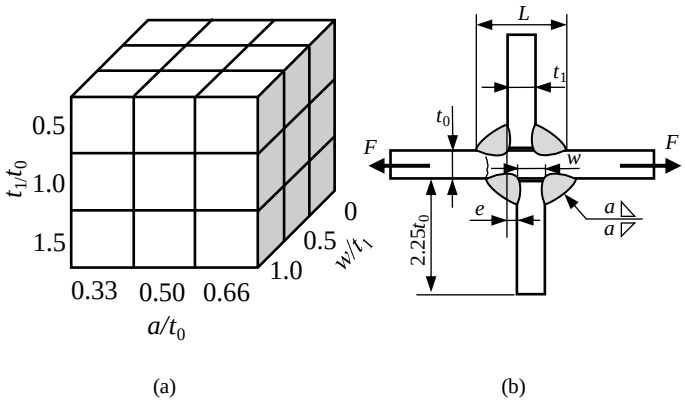

Fig. 8. (a) Analyzed geometry combinations, and (b) dimensions of the joint.

2.2.3 Linear elastic fracture mechanics

2D LEFM analyses were carried out to evaluate the effect of misalignment on the fatigue strength prediction using a crack propagation-based analysis. In the conducted experiments, no initial defects or flaws, such as cold laps or sharp undercuts, were present, but LEFM analysis provides an insight into the results for NLCX joints with initial flaws. In addition, when considering the crack propagation of the studied joint types, it is noticeable that the early crack propagation is influenced by the presence of a notch induced by the weld toe. Whereas for large fatigue cracks, general stress state and crack shape dominates the crack propagation.

Numerical analyses were carried out using the Franc2D software provided by Cornell University [37]. 2D element meshes of the studied NLCX joints were modeled, corresponding to the geometry presented in Section 2.2.1, see Fig. 9a. However, for the sake of similarity with the fatigue tested joints, a weld toe radius was modeled according to the measured average weld toe radius, $r_{true,avg}$ = 0.3 mm. For the design purposes, IIW recommends an initial crack depth of a_i = 0.1 mm for sharp notches. In the FE modeling, crack of 0.025 mm was applied to the model, see Fig. 9b, which was subsequently propagated to achieve an initial crack depth of 0.1 mm. From a fatigue life viewpoint, the final crack depth does not have a major effect on the results. In this case, the final

crack depth was a_f = 7 mm, i.e. a_f/t = 0.875, to confirm the stability of FE re-meshing when reaching the plate surface. The crack path was obtained using the maximum tangential stress criterion. A seed load of 1 MPa was used in the model, and afterwards multiplied with the stress range corresponding to the test load, see Table 5 in Section 3.1.

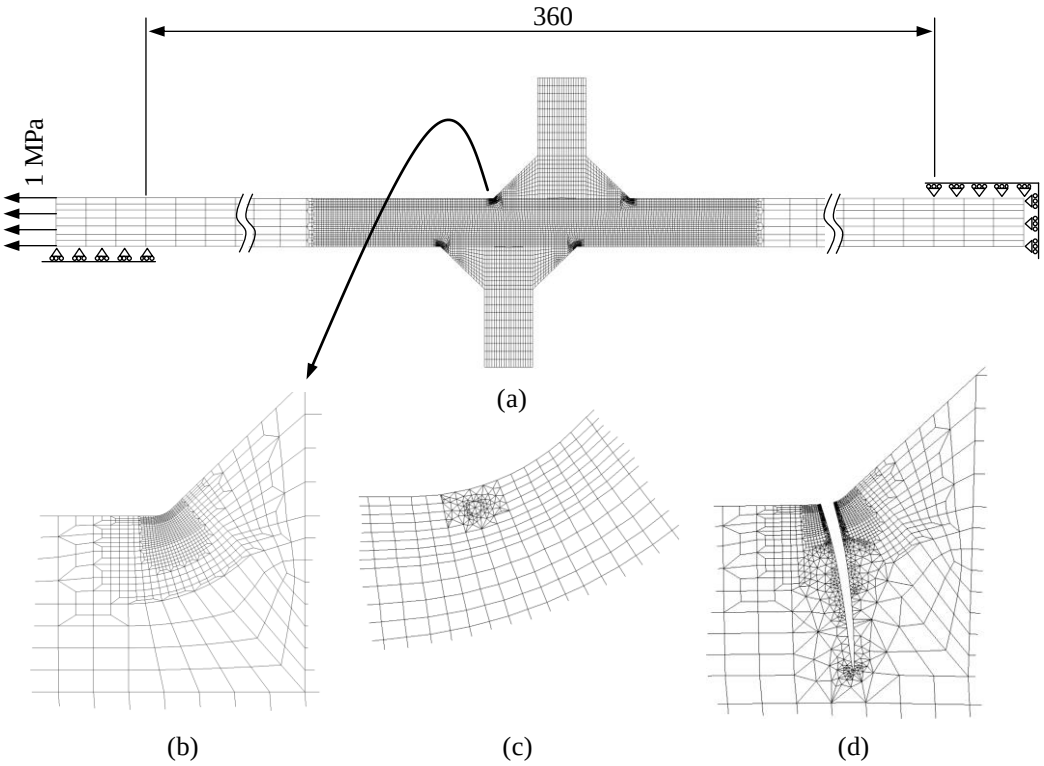

Fig. 9. 2D LEFM models: (a) full model with boundary conditions, (b) detailed view of the weld toe mesh, (c) initial crack of a_i = 0.025 mm, and (d) a propagated crack with the depth of a = 1.5 mm.

From the LEFM models, the SIF values (K_I and K_{II}) were obtained using a J-integral approach embedded in the software. The magnitude of K_{II} values is negligibly low in this case with respect to K_I values, so it can be ignored when assessing fatigue life. The crack propagation fatigue life can be obtained using Paris' law:

$$\frac{da}{dN} = C\left(\Delta K(a)\right)^m, \tag{2}$$

where a is crack depth, N is the number of cycles, C is the crack propagation coefficient, $\Delta K(a)$ is the SIF as a function of crack depth, and m is the slope of Paris' law.

3 RESULTS

3.1 Fatigue test results

A total number of 14 NLCX specimens, including six reference specimens without plate misalignment, and eight specimens with misalignment, were fatigue tested using uniaxial loading with an applied stress ratio of R = 0.1. All specimens failed at the weld toe, and, in the case of misaligned NLCX, the specimens failed at the inner weld toe, as shown in Fig. 10, due to the stress concentration induced by the plate misalignment. Numerical analyses were conducted, see Section 2.2, to obtain SCF for different stress criteria, i.e. structural HS stress using the LSE and Xiao–Yamada methods, together with the ENS approach with the reference radius of r_{ref} = 1.0 mm.

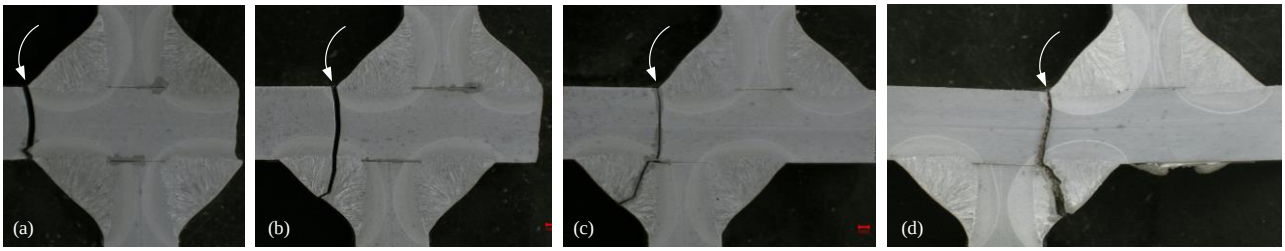

Fig. 10. Fatigue failures of the test specimens: (a) a reference specimen (S11_NLCX_1), (b) e = 6 mm, (c) e = 9 mm, and (d) e = 16 mm. White arrows show the weld toe location of an initiated fatigue crack.

Table 5 summarizes the fatigue testing details, and Fig. 11 shows the fatigue data plots and obtained mean fatigue strength and scatter ranges values in a log-log coordinate system in comparison with the standard curves using different stress criteria, i.e. the nominal stress, structural HS stress (LSE and 1 mm depth methods), and ENS approaches. In the nominal stresses, the macrogeometric stresses induced by the angular distortions were also considered.

Table 5. Results of fatigue testing.

ID	e [mm]	$\Delta\sigma_{nom}$ [MPa]	$K_{s,m,\mathrm{LSE}}$ [-]	$K_{s,m,1\mathrm{mm}}$ [-]	$K_{tot,m}$ [-]	$N_{f,exp}$ [cycles]
S11_NLCX_1	0	312	1.0	1.0	2.30	72 872
S11_NLCX_2	0	317	1.0	1.0	2.30	82 578
S11_NLCX_3	0	247	1.0	1.0	2.30	169 415
S11_NLCX_4	0	241	1.0	1.0	2.30	169 322
S11_NLCX_5	0	205	1.0	1.0	2.30	496 828
S11_NLCX_6	0	196	1.0	1.0	2.30	528 328
S11_NLCX_13	6	206	1.37	1.17	2.85	214 769
S11_NLCX_14	6	168	1.37	1.17	2.85	547 795
S11_NLCX_15	9	206	1.48	1.17	2.74	217 244
S11_NLCX_16	9	244	1.48	1.17	2.74	124 297
S11_NLCX_17	9	169	1.48	1.17	2.74	596 207
S11_NLCX_18	9	188	1.48	1.17	2.74	463 560
S11_NLCX_19	16	206	1.34	1.12	2.48	253 715
S11_NLCX_20	16	168	1.34	1.12	2.48	883 148

Using a free slope parameter and standard statistical evaluation of *S-N* curves, the mean fatigue strength can be evaluated for each series (misalignments of e = 0, 6, 9 and 16 mm). First, the slope parameters of *S-N* curves are evaluated for all data points, subsequently, the mean fatigue strength at two million cycles with a survival probability of P_s = 50% is obtained for each series, see Fig. 12. The characteristic design curves (P_s = 97.7%) were not obtained within this study due to the low number of test specimens in the experimental program.

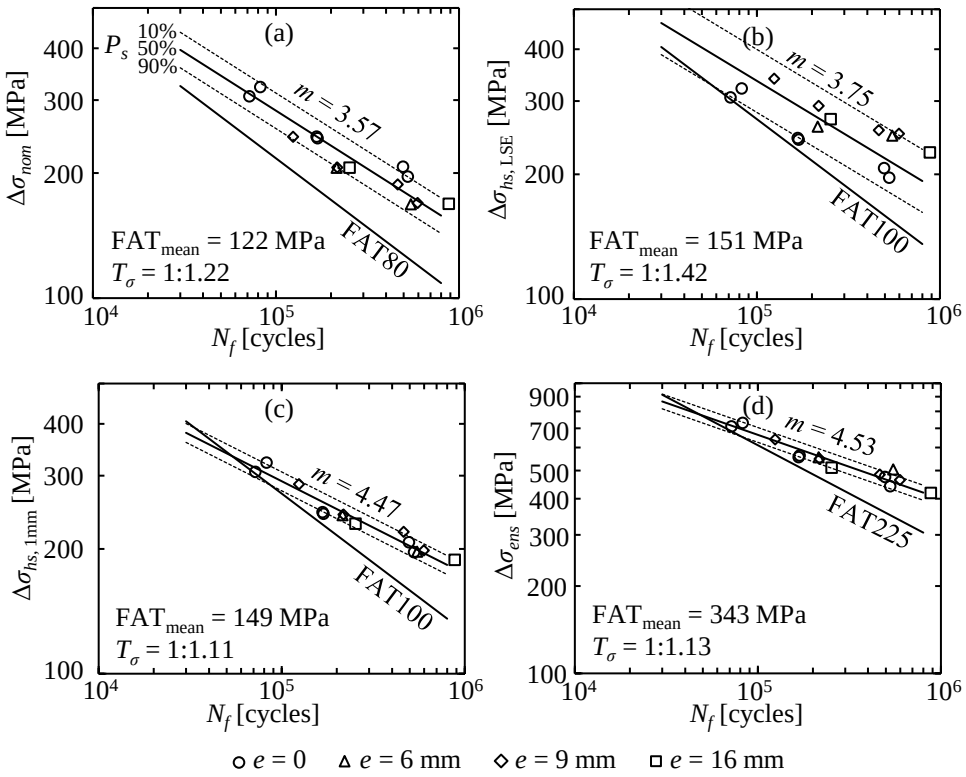

Fig. 11. *S-N* data plots using different stress criterion: (a) nominal stress, (b) structural HS stress using the LSE method, (c) structural HS stress using the Xiao-Yamada 1 mm depth stress, and (d) the ENS concept. All standardized reference *S-N* curves (characteristic, P_s = 97.7%) have a slope parameter of m = 3 [7]. FAT is the fatigue strength (in MPa) at two million cycles.

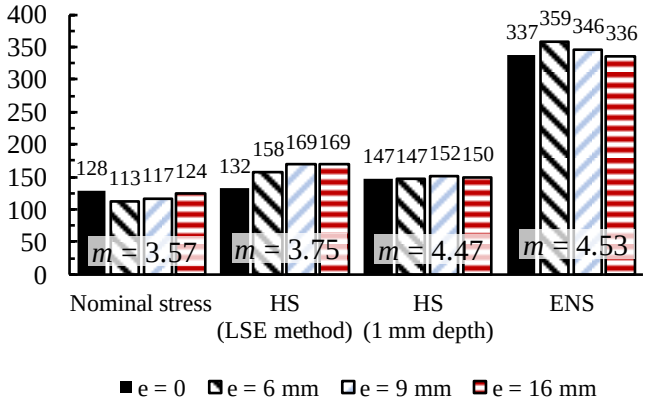

Fig 12. Experimental mean fatigue strength (P_s = 50%) value for different stress criteria using a free slope parameter of the *S-N* curve.

The angular distortions due to the welding were negligibly low and, consequently, no bending stress was present in the fatigue tests, and strain gages were not always positioned in the vicinity of failing weld toe. However, Fig. 13 exemplifies the strain gage measurements in the fatigue tests where strain gage was next to the failing weld toe. Based on the changes in the strain range $\Delta\varepsilon$, the crack initiation (CI) and crack propagation (CP) periods can be estimated.

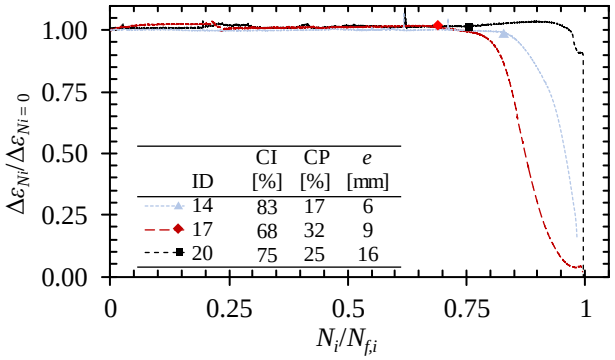

Fig. 13. Strain gage measurements during the fatigue tests: CI and CP periods of the total fatigue life, based on the strain drop at weld toe having a fatigue crack.

3.2 Stress distributions and stress concentration factors

Numerical analyses were conducted to evaluate the stress concentration factors induced by the plate misalignment. Fig. 14 exemplifies the normal stress distributions at plate surfaces in the NLCX joint with equal plate thicknesses ($t_1 = t_0 = 8$ mm), and with a throat thickness of $a = 4$ mm. The structural stresses, obtained using the LSE method (type 'a'), are extrapolated at the given points. Fig. 14c shows that the inner and outer weld toe have identical notch stress but, due to the stress distribution at joint area, the LSE method estimates a structural SCF of less than 1.

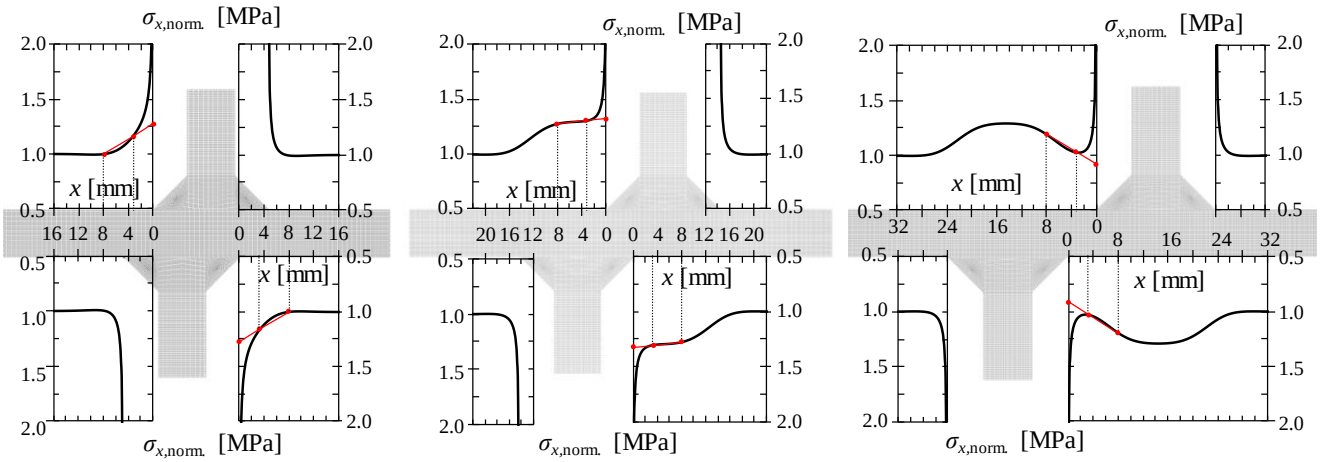

Fig. 14. Normalized normal stress ($\sigma_{x,\text{norm.}}$) distributions of the misaligned NLCX joints obtained using FEA: (a) e/L = 0.25, (b) e/L = 0.75 and (c) e/L = 1.25.

To determine the effect of geometrical parameters, i.e. plate thickness (t_1/t_0), throat thickness (a/t_0), and degree of weld penetration (w/t_1) on the magnitude of SCF, parametric analyses were carried out. Fig. 15 summarizes the results of structural SCFs determined using the applied structural stress methods, and Fig. 16 presents the results of SCFs obtained using r_{ref} = 1.0 mm, i.e. the ENS method denoted with K_{tot}, including both the structural stress and notch effect.

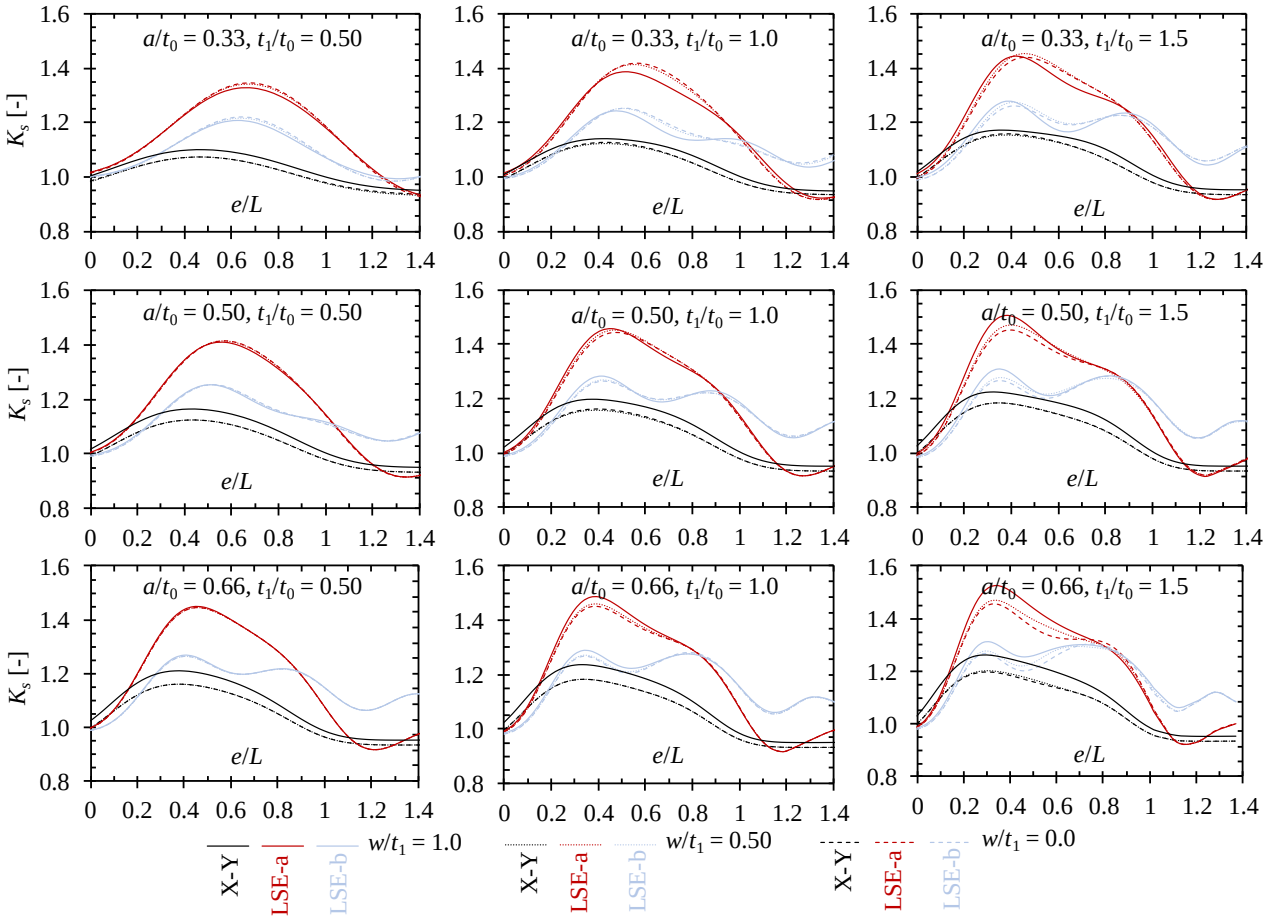

Fig. 15. Results of parametric analyses: structural SCFs obtained using the Xiao–Yamada (X-Y) method (1 mm below depth), 'a' type of LSE (LSE-a), and 'b' type of LSE (LSE-b).

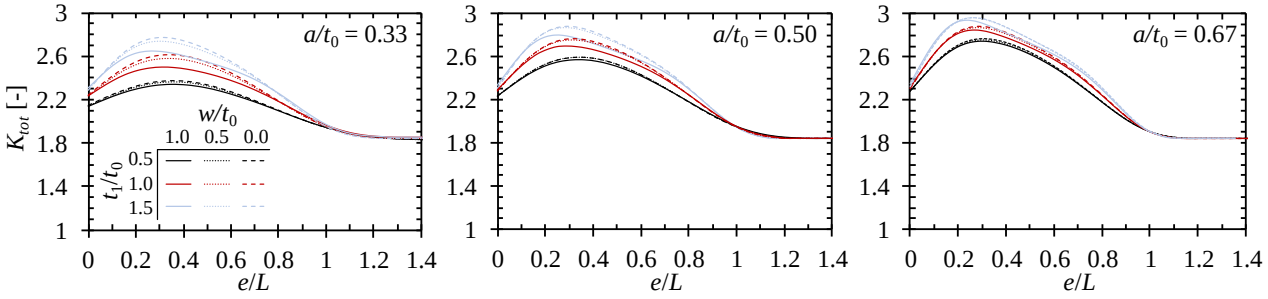

Fig. 16. Results of parametric analyses: SCFs in terms of the ENS system.

3.3 Fatigue strength predictions

This section summarizes the numerical results obtained to evaluate the structural behavior of misaligned NLCX joints, as well as to predict the fatigue strength of such joints using different fatigue

strength assessment approaches in comparison with the experimental fatigue test results. Table 6 presents the reference *S-N* curves of each stress-based fatigue strength assessment method and the crack propagation coefficients for LEFM. In both cases, the values are representative of characteristic values with the survival probability of P_s = 97.7%. Fig. 17 shows the predicted computational fatigue lives with respect to the experimental results.

Table 6. Characteristic model parameters for different fatigue strength assessment approaches (units are in mm, MPa and N). C_{4R} is the fatigue capacity for the 4R method, σres is the residual stress, r is the weld toe radius applied in the FE model, H and n are the strain hardening coefficient and exponent, respectively, and C is the crack propagation coefficient.

Approach	Parameters	Ref.
Nominal stress	FAT80, m = 3	[7,38]
Structural HS stress	FAT100, m = 3	[7]
ENS	FAT225, m = 3	[7]
4R	$C_{4R} = 10^{17.94}$, m = 4.65	[33]
	σ_{res} = 0, R = 0.1, r = 1.3 mm	
	H = 1391 MPa, n = 0.03	
LEFM	$C = 3.0 \cdot 10^{-13}$*, m = 3,	[7]
	a_i = 0.1 mm	

* Based on the prior value. The current more conservative estimation is $C = 5.21 \cdot 10^{-13}$.

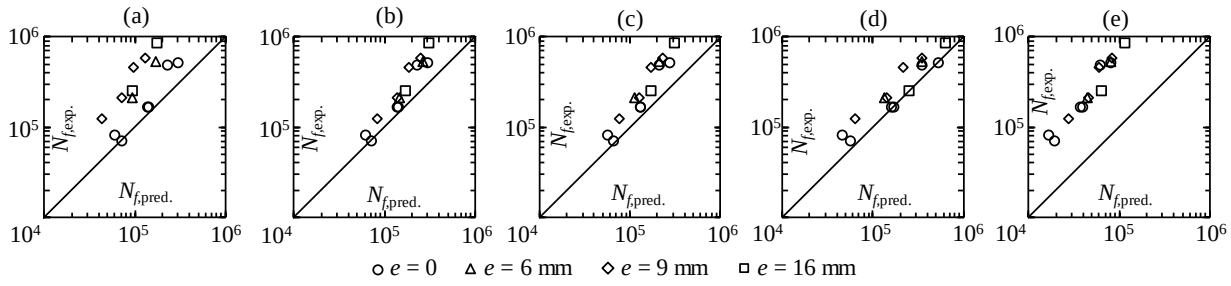

Fig. 17. Fatigue test results in comparison with predicted fatigue lives: (a) HS with LSE method, (b) Structural stress method using stress at 1 mm depth, (c) ENS method, (d) 4R method, and (e) LEFM.

4 DISCUSSION

In the present study, the effect of plate misalignment on the fatigue performance of fillet-welded NLCX joints was evaluated by conducting experimental fatigue tests for NLCX fillet weld joints

made of t = 8 mm S1100 UHSS grade. In addition, numerical analyses were carried out to investigate the stress concentrations induced by the misaligned, and the effect of geometry parameters (plate and throat thickness, and weld penetration) on the magnitude of SCFs, and to investigate the degree of misalignment (e/L ratio) inducing the maximum SCF. The SCFs were investigated using the structural HS stress-based methods, determined using the LSE method and Xiao–Yamada method [31], and the ENS method with the reference radius of r_{ref} = 1.0 mm. In addition, the fatigue life predictions were conducted with a multiparametric notch stress-based approach, the 4R method, and LEFM.

In prior investigations related to the topic [25,26], a low degree of misalignment was investigated by the fracture mechanics-based evaluation, and, in those studies, only minor effects on the fatigue life were found. As shown in this study, the maximum SCF (K_{tot}) is induced when the misalignment to the joint width ratio is e/L = 0.2–0.4, see Figs. 15–16. Consequently, the fatigue strength is influenced by the misalignment. Experimental fatigue tests showed a decrease of 12% in fatigue strength for the misaligned joint compared to the joint without misalignment (corresponding to 36% in fatigue life) when using the nominal stress approach. Depending on the joint geometry, the maximum stress concentration induced by the misalignment is derived when the degree of misalignment is e/L = 0.2–0.4. As shown in a prior investigation [28], fillet-welded single-sided non-load carrying transverse (NLCT) joint has a lower notch SCF than a double-sided NLCX joint, which was also clearly indicated by this study as, when e/L > 1.0, the notch SCF for T joint is 80%–85% of the corresponding notch SCF of X joint, see Fig. 16. It is also worth noting that, in the case of T joint (e/L > 1.0), the joint geometry parameters do not have influence on the notch SCF; K_{tot} = 1.84 was derived for all geometries, while for the X joints (e/L = 0), the notch SCF depends on the joint geometry (throat thickness, the thickness of adjoined plate component, and weld penetration). The results of this study can also reflect on, for instance, welding-repaired fatigue cracks in welded components [39]; as the weld toes are not aligned after repairing, in axial loading the outer weld toe has lower stress concentration, as also demonstrated in Fig. 18.

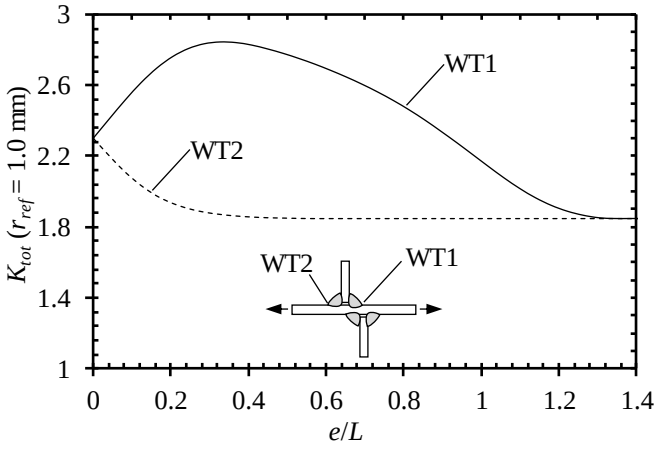

Fig. 18. Comparison of notch SCFs at outer and inner weld toes (WTs) for the tested specimens.

When observing the applicability of local stress-based approaches for evaluating the effect of plate misalignment on the fatigue performance of the fillet welded NLCX joints, it was clearly indicated that the LSE method with extrapolation points (type 'a' or type 'b') is not able to evaluate the structural SCF correctly, because the extrapolation points are influenced by the through-thickness stress distribution of the adjacent (outer) weld toe. Consequently, more local approaches are needed for the fatigue analysis of misaligned joints. In this study, a structural stress method using stress value at the 1 mm depth after Xiao and Yamada [31], and the ENS concept were utilized in the fatigue assessments. Both methods showed good agreement with the experimental results, i.e. similar fatigue strengths were obtained for different misalignment degrees, see Fig. 12. However, it is worth noting that the magnitude of structural stress at the 1 mm depth is significantly influenced by the stress distribution in through-thickness direction, and for thicker or thinner plates the stress distribution is different.

Fig. 19 summarizes the fatigue test results in comparison with applied fatigue strength assessment approaches. The effect of plate misalignment is evaluated by comparing the fatigue strength of a misaligned ($e/L > 0$) NLCX joint to an NLCX joint without misalignment ($e/L = 0$) in terms of nominal stress applied in the base plate. In this regard, an LEFM-based evaluation on the plate misalignment effects gives the closest estimation with respect to the experimental result but, on

the other hand, offers very conservative estimations for fatigue life, as clearly demonstrated in Fig. 17e, while Fig. 19 provides the proportional comparison of fatigue strengths only. When comparing the fatigue life predictions using different approaches, the notch-stress based system, the ENS method and particularly the 4R method all showed a good correspondence between the experimental lives, Fig 17.

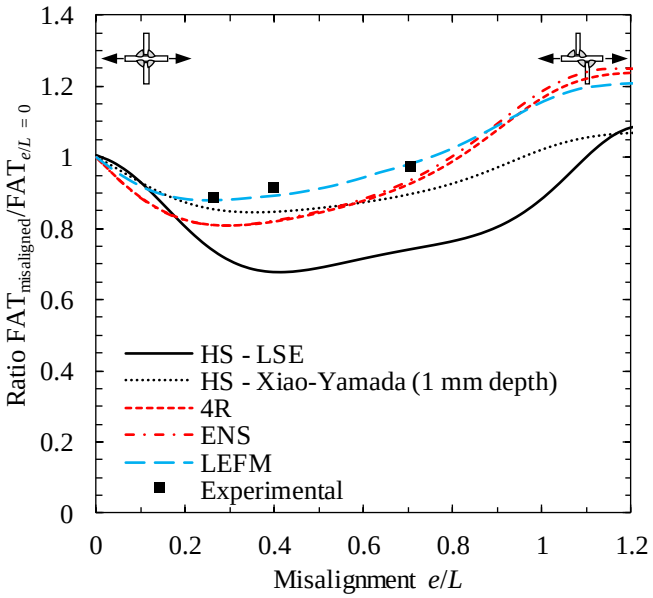

Fig. 19. Comparison of the effect of plate misalignment on the fatigue strength capacity converted to the nominal stress system.

In the experiments of the present study, a robotized GMAW was employed to produce constant welding quality through all test welds and fatigue test specimens to diminish the effect of changes in weld geometry easily produced by manual welding. The changes in weld size alter the degree of misalignment along the weld, and the changes in local weld toe geometry have a significant influence on the notch stress concentration that may disable concluding the effects of misalignment. Nevertheless, the weldments of this study were prepared at the PB position (horizontal plate in the loading direction, see Fig. 4) and, consequently, quite a sharp transition was produced, i.e. $r_{true,\,avg}$ = 0.3 mm. This signifies a rather sharp notch but, however, no initial fatigue crack was present at the

weld toe, and the major share of total fatigue life, up to 80%, was comprised of the fatigue crack initiation period, as demonstrated in Fig. 13. Reflecting on the prior investigations of crack initiation share, the result is quite typical for welded UHSS joints [28,29]. By changing the welding procedure, or implementing post-weld treatments, the fatigue performance of weld toes in UHSS joints can be significantly improved [40,41], and the fatigue life is even more controlled by the local notch stress. Consequently, further experiments should be conducted for various weld toe qualities and applied stress ratios, and considerations made on the effect of plate misalignment on the fatigue strength of misaligned joints in the case of bending load.

5 CONCLUSIONS

In the present study, the fatigue strength of axially loaded misaligned thin-walled (t = 8 mm) NLCX joints was evaluated experimentally by conducting fatigue tests on NLCX joints made of S1100 UHSS material, and numerically conducting FEAs to determine the SCFs induced by the misalignments. Based on the results of the numerical and experimental studies, the following conclusions can be drawn:

- In the misaligned fillet-welded NLCX joints, the inner weld toe is the fatigue critical weld toe under axial cyclic loading, not the outer one due to stress concentration induced at the inner weld toe (see experimental fatigue failures in Fig. 10 and stress distributions in Fig. 14);
- The fatigue strength of NLCX joints decreases by up to 12% when a plate misalignment of adjoined plate components occurs. The maximum SCF occurs when the misalignment to joint width ratio is e/L = 0.2–0.4, while the misaligned joint has a lower SCF when the misalignment is more than e/L = 0.6–0.8, as the NLCT joints have lower notch SCF than the corresponding NLCX joints in axial loading;
- An increase in the plate thickness of the adjoined plate component or throat thickness results in higher magnitude of misalignment effect on the SCF. The degree of weld penetration has a

negligibly small effect on the SCF, particularly in the case of the small plate thickness of adjoined plate component or large throat thickness;

- Notch stress-based methods seem to be applicable for evaluating the effect of plate misalignment on the fatigue performance of misaligned fillet-welded NLCX joint – a scatter range value of T_σ = 1:1.13 was found. A structural HS approach using the LSE method is not applicable for evaluating the SCF as the stress values at the extrapolation points are affected by the notch stress distribution of adjacent notch detail (see Fig. 11b and Fig. 14).

ACKNOWLEDGEMENTS

This work was supported by Business Finland in the Intelligent Steel Applications (ISA) project (Grant ID: 7386/31/2018). Furthermore, the authors wish to thank SSAB Europe for their funding of experimental fatigue testing.

REFERENCES

[1] H. Ban, G. Shi, A review of research on high-strength steel structures, Struct. Build. 171 (2018).

[2] C. Miki, K. Homma, T. Tominaga, High strength and high performance steels and their use in bridge structures, J. Constr. Steel Res. 58 (2002) 3–20. doi:10.1016/S0143-974X(01)00028-1.

[3] C.M. Sonsino, Light-weight design chances using high-strength steels, Mater. Sci. Eng. Technol. 38 (2007) 9–22. doi:10.1002/mawe.200600090.

[4] A.M.P. De Jesus, R. Matos, B.F.C. Fontoura, C. Rebelo, L. Simões Da Silva, M. Veljkovic, A comparison of the fatigue behavior between S355 and S690 steel grades, J. Constr. Steel Res. 79 (2012) 140–150. doi:10.1016/j.jcsr.2012.07.021.

[5] P.J. Haagensen, S.J. Maddox, IIW Recommendations on Methods for Improving the Fatigue Strength of Welded Joints, Woodhead Publishing, 2013.

[6] G.B. Marquis, Z. Barsoum, IIW Recommendations for the HFMI Treatment - For Improving

the Fatigue Strength of Welded Joints, Springer Singapore, Singapore, 2016. doi:10.1007/978-981-10-2504-4.

[7] A. Hobbacher, Recommendations for Fatigue Design of Welded Joints and Components, 2nd ed., Springer International Publishing, Cham, 2016.

[8] DNVGL-RP-C203, Fatigue Design of Offshore Steel Structures, 2016.

[9] BS7608:2014 +A1:2015, Guide to Fatigue Design and Assessment of Steel Products, 2015.

[10] L. Eggert, W. Fricke, H. Paetzold, Fatigue strength of thin-plated block joints with typical shipbuilding imperfections, Weld. World. 56 (2012). doi:10.1007/BF03321402.

[11] I. Lotsberg, Stress concentrations due to misalignment at butt welds in plated structures and at girth welds in tubulars, Int. J. Fatigue. 31 (2009) 1137–1345. doi:10.1016/j.engfailanal.2016.11.006.

[12] H. Remes, W. Fricke, Influencing factors on fatigue strength of welded thin plates based on structural stress assessment, Weld. World. 58 (2014) 915–923. doi:10.1007/s40194-014-0170-7.

[13] A.J. Pachoud, P.A. Manso, A.J. Schleiss, New parametric equations to estimate notch stress concentration factors at butt welded joints modeling the weld profile with splines, Eng. Fail. Anal. 72 (2017) 11–24. doi:10.1016/j.engfailanal.2016.11.006.

[14] M. Dabiri, M. Ghafouri, H. Rohani Raftar, T. Björk, Utilizing artificial neural networks for stress concentration factor calculation in butt welds, J. Constr. Steel Res. 138 (2017) 488–498. doi:10.1016/j.jcsr.2017.08.009.

[15] M.J. Ottersböck, M. Leitner, M. Stoschka, W. Maurer, Analysis of fatigue notch effect due to axial misalignment for ultra high-strength steel butt joints, Weld. World. 63 (2019) 851–865. doi:10.1007/s40194-019-00713-4.

[16] H. Jakubczak, G. Glinka, Fatigue analysis of manufacturing defects in weldments, Int. J. Fatigue. 8 (1986) 51–57. doi:10.1016/0142-1123(86)90053-8.

[17] M.Skorupa, Fatigue life prediction of cruciform joints failing at the weld toe, Weld. Res.

(1992) 269–276.

[18] R.M. Andrews, The effect of misalignment on the fatigue strength of welded cruciform joints, Fatigue Fract. Eng. Mater. Struct. 19 (1996) 755–768. doi:10.1111/j.1460-2695.1996.tb01320.x.

[19] R. Goyal, G. Glinka, Fracture mechanics-based estimation of fatigue lives of welded joints, Weld. World. 57 (2013) 625–634. doi:10.1007/s40194-013-0060-4.

[20] S. Xing, P. Dong, P. Wang, A quantitative weld sizing criterion for fatigue design of load-carrying fillet-welded connections, Int. J. Fatigue. 101 (2017) 448–458. doi:10.1016/j.ijfatigue.2017.01.003.

[21] C. Cui, Q. Zhang, Y. Bao, J. Kang, Y. Bu, Fatigue performance and evaluation of welded joints in steel truss bridges, J. Constr. Steel Res. 148 (2018) 450–456. doi:10.1016/j.jcsr.2018.06.014.

[22] Y. Dong, C.G. Soares, On the fatigue crack initiation point of load-carrying fillet welded joints, in: C. Guodes Soares, R. Dejhalla, D. Pavletic (Eds.), Towar. Green Mar. Technol. Transp., 2015: pp. 407–416. doi:10.1201/b18855.

[23] A. Ahola, T. Björk, Z. Barsoum, Fatigue strength capacity of load-carrying fi llet welds on ultra-high-strength steel plates subjected to out-of-plane bending, Eng. Struct. 196 (2019) 109282. doi:10.1016/j.engstruct.2019.109282.

[24] R. Ghafoori-Ahangar, Y. Verreman, Fatigue behavior of load-carrying cruciform joints with partial penetration fillet welds under three-point bending, Eng. Fract. Mech. 215 (2019) 211–223. doi:10.1016/j.engfracmech.2019.05.015.

[25] L. Zong, G. Shi, Y.Q. Wang, Z.X. Li, Y. Ding, Experimental and numerical investigation on fatigue performance of non-load-carrying fillet welded joints, J. Constr. Steel Res. 130 (2017) 193–201. doi:10.1016/j.jcsr.2016.12.010.

[26] H. Su, J. Wang, J. Du, Fatigue behavior of uncorroded non-load-carrying bridge weathering steel Q345qDNH fi llet welded joints, J. Constr. Steel Res. 164 (2020) 105789.

doi:10.1016/j.jcsr.2019.105789.

[27] M.M.P. Mbeng, Effective notch method assessment of misalignment for fatigue loaded welds. Master's thesis, Lappeenranta University of Technology, 2007.

[28] A. Ahola, T. Nykänen, T. Björk, Effect of loading type on the fatigue strength of asymmetric and symmetric transverse non-load carrying attachments, Fatigue Fract. Eng. Mater. Struct. 40 (2017) 670–682. doi:10.1111/ffe.12531.

[29] M.J. Ottersböck, M. Leitner, M. Stoschka, W. Maurer, Crack initiation and propagation fatigue life of ultra high-strength steel butt joints, Appl. Sci. 9 (2019). doi:10.3390/app9214590.

[30] E. Niemi, W. Fricke, S.J. Maddox, Structural Hot-Spot Stress Approach to Fatigue Analysis of Welded Components, 2nd editio, Springer Singapore, Singapore, 2017. doi:10.1007/978-981-10-5568-3.

[31] Z.G. Xiao, K. Yamada, A method of determining geometric stress for fatigue strength evaluation of steel welded joints, Int. J. Fatigue. 26 (2004) 1277–1293. doi:10.1016/j.ijfatigue.2004.05.001.

[32] C.M. Sonsino, W. Fricke, F. De Bruyne, A. Hoppe, A. Ahmadi, G. Zhang, Notch stress concepts for the fatigue assessment of welded joints - Background and applications, Int. J. Fatigue. 34 (2012) 2–16. doi:10.1016/j.ijfatigue.2010.04.011.

[33] A. Ahola, T. Skriko, T. Björk, Fatigue strength assessment of ultra-high-strength fillet weld joints using 4R method (in press), J. Constr. Steel Res. (2019). doi:10.1016/j.jcsr.2019.105861.

[34] T. Skriko, M. Ghafouri, T. Björk, Fatigue strength of TIG-dressed ultra-high-strength steel fillet weld joints at high stress ratio, Int. J. Fatigue. 94 (2017) 110–120. doi:10.1016/j.ijfatigue.2016.09.018.

[35] E. Niemi, W. Fricke, S.J. Maddox, Fatigue Analysis of Welded Components: Designer's Guide to the Structural Hot-Spot Stress Approach, 2nd editio, Springer Nature, Singapore, 2018. doi:10.1533/9781845696665.

[36] J. Baumgartner, T. Bruder, An efficient meshing approach for the calculation of notch stresses,

Weld. World. 57 (2013) 137–145. doi:10.1007/s40194-012-0005-3.

[37] Cornell Fracture Group, Software, (2020). http://cfg.cornell.edu/software/ (accessed January 9, 2020).

[38] EN 1993-1-9, Eurocode 3 - Design of steel structures - Part 1-9: Fatigue, 2005.

[39] J. Schubnell, A. Sarmast, E. Carl, M. Farajian, P. Ladendorf, P. Knödel, T. Ummenhofer, Fatigue performance of repaired welded joints made of S355 and S960 steel, in: 72nd IIW Annu. Assem. Int. Conf. - Comm. XIII - WG2, 2019.

[40] J. Berg, N. Stranghöner, Fatigue behaviour of high frequency hammer peened ultra high strength steels, Int. J. Fatigue. 82 (2016) 35–48. doi:10.1016/j.ijfatigue.2015.08.012.

[41] A. Ahola, T. Skriko, T. Björk, Experimental investigation on the fatigue strength assessment of welded joints made of S1100 ultra-high-strength steel in as-welded and post- weld treated condition, in: 7 Th Int. Conf. Struct. Eng. Mech. Comput., Cape Town, South Africa, 2019: pp. 1–6.